Quantification of cerebral hemoglobin as a function of oxygenation using near-infrared time-resolved spectroscopy in a piglet model of hypoxia

Sonoko Ijichi
Kagawa University
Department of Pediatrics
Faculty of Medicine
Mikicho 1750-1
Kitagun, Kagawa 761-0793, Japan

Takashi Kusaka
Kagawa University
Maternal and Perinatal Center
Faculty of Medicine
Mikicho 1750-1
Kitagun, Kagawa 761-0793, Japan
E-mail: kusaka@ kms.ac.jp

Kenich Isobe
Fahmida Islam
Kensuke Okubo
Hitoshi Okada
Masanori Namba
Kagawa University
Department of Pediatrics
Faculty of Medicine
Mikicho 1750-1
Kitagun, Kagawa 761-0793, Japan

Kou Kawada
Kagawa University
Maternal and Perinatal Center
Faculty of Medicine
Mikicho 1750-1
Kitagun, Kagawa 761-0793, Japan

Tadashi Imai
Susumu Itoh
Kagawa University
Department of Pediatrics
Faculty of Medicine
Mikicho 1750-1
Kitagun, Kagawa 761-0793, Japan

Abstract. Near-infrared spectroscopy (NIRS) has been used for measurement of cerebral hemoglobin (Hb) concentrations in neonates to study cerebral oxygenation and hemodynamics. We perform measurements by portable three-wavelength NIR time-resolved spectroscopy (TRS) in a piglet hypoxia model with various degrees of oxygenation to estimate the absorption coefficient (μ_a) and reduced scattering coefficient (μ_s') of the head. Measurements of absolute values of μ_a at three wavelengths enable estimation of Hb concentration and Hb oxygen saturation in the head (SO_2). However, there is a problem concerning which background absorption should be used to estimate Hb concentration in the head derived from μ_a at three wavelengths because it is different from a simple *in vitro* model. Therefore, we use two different background absorption values with the assumption that background absorption is due only to 85% (by volume) water or that background absorption is equal to absorption of the piglet head with blood exchange transfusion by fluorocarbon (FC), and we compared SO_2 measured by TRS with arterial Hb oxygen saturation (SaO_2) and sagittal sinus venous Hb oxygen saturation (SvO_2) measured by a co-oximeter at several inspired fractional O_2(FI_{O_2}) concentrations. We find that SO_2 values using the absorption (abs) of the piglet head with blood exchange transfusion (BET) by FC are not significantly different from SO_2 values using the water-only background at FI_{O_2} in the range of 15 to 100%, but that the values using abs of the head with BET by FC are lower than the values using the water-only background at FI_{O_2} in the range of 12 to 4%. The SO_2 values calculated from the water-only background are higher than those of SaO_2 at FI_{O_2} in the range of 10 to 4%. However, SO_2 values using the abs of the head with BET by FC are between those of SaO_2 and SvO_2 over the whole range of FI_{O_2}. Therefore, abs of the head with BET by FC is more useful for estimation of the absolute values of oxyHb and deoxyHb of the piglet head. [DOI: 10.1117/1.1899184]

Keywords: background absorption; cerebral hemoglobin concentration; cerebral hemoglobin oxygen saturation; fluorocarbon; hypoxia; near-infrared spectroscopy; newborn piglets; time-resolved spectroscopy.

Paper 03132 received Nov. 12, 2003; revised manuscript received Apr. 21, 2004; accepted for publication Sep. 10, 2004; published online Apr. 22, 2005.

1 Introduction

Near-IR spectroscopy (NIRS), which uses light in the NIR range (700 to 900 nm), enables detection of changes in the oxygenation state of hemoglobin (Hb) and water in biological tissues. Several studies have shown the usefulness of NIRS for noninvasive measurement of cerebral blood volume and oxygenation in infants.[1–7]

A number of approaches for measuring cerebral Hb concentration and oxygen saturation using several types of NIRS systems have been proposed. These approaches include (1) continuous wave spectroscopy (CWS), by which only the relative value of Hb can be estimated;[8] (2) full spectral spectroscopy (FSS), by which the NIR full spectrum of the NIR range can be measured;[9–12] (3) time-resolved spectroscopy (TRS), by which the transit time of each photon through the tissue of interest can be measured;[13–18] (4) phase-modulated spectroscopy (PMS), by which amplitude signals for phase,

Address all correspondence to Takashi Kusaka, Kagawa Medical University, Department of Pediatrics, 1750-1 Ikenobe, Mikicho, Kilagun, Kagawa 761-0793, Japan.

1083-3668/2005/$22.00 © 2005 SPIE

intensity and depth of modulation after passage can be measured;[19–25] and (5) spatially resolved spectroscopy, by which the slope of light attenuation versus distance is determined at a distant point from the source.[26]

A new TRS system that is portable and has a high data acquisition rate was recently reported.[18,27,28] A TRS device enables quantitative analysis of light absorption and scattering in tissue using the photon diffusion theory. The absorption coefficient (μ_a) represents the physiological state, particularly the Hb concentration and oxygen saturation, and the reduced scattering coefficient (μ_s') represents the structural change in tissue. However, for application to tissue measurements, there is the problem concerning how to determine the background absorption for estimation of Hb in the head. Hueber et al.[24] reported the use of fixed weighted averages of SaO_2 and SvO_2 for estimation of background tissue absorption using PMS. However, an exact background absorption has not been reported.

In this paper, we first investigate whether our TRS measurements could be used to accurately measure Hb concentration and oxygen saturation in an *in vitro* model such as the brain. Next, we apply this method to newborn piglets during hypoxic loading. In this experiment, we use two different methods to determine Hb concentration and oxygen saturation in the head using μ_a values measured at three wavelengths. One method uses a water-only background absorption to determine the Hb concentration, and we investigate the relationships of cerebral Hb oxygenation with arterial and sagittal sinus venous Hb oxygen saturation at various concentrations of inspired oxygen using a piglet hypoxic model. Another method uses background absorption from the piglet head with blood exchange by fluorocarbon (FC), and we reestimate cerebral Hb concentration for comparison to that with water-only background absorption calculations. Then the reliability of the instruments is evaluated. The results of optical path length obtained in this study were previously published.[27]

2 Materials and Methods

2.1 *In Vitro Experimental Protocol*

To provide a model for *in vivo* measurement of Hb in the piglet brain, we filled a 1.000-mL glass beaker with 0.1-M phosphate buffer (*p*H 7.4) containing 0.7% (w/vol) dry yeast in 1% intralipid and glucose (2% w/vol) to produce a solution with a light scattering condition equivalent to that of blood-perfused brain tissue. A magnetic stirrer was used to prevent particle settling. The measurement receiver fiber was set at a distance of 30 mm from the light source fiber, and the fibers were immersed directly in the suspension. The oxygen content was also monitored at the same time with a conventional gas analyzer (ABL5, Radiometer, Copenhagen, Denmark). In the first stage of the experiment, human blood was added gradually to the beaker to achieve blood volume ranging from 0 to 100 μM, and the resulting changes in the reemission profiles were recorded. Each model was bubbled with oxygen. In the second stage of the experiment, we used a model solution with a 80-μM Hb suspension, and the oxygen concentration in the solution was reduced to simulate anoxia in the brain. A mixture of O_2 and N_2 gases was prepared and bubbled through the suspension to manipulate the oxygen saturation of Hb from 0 to 100%.

Once μ_a had been determined at three wavelengths, the oxyHb and deoxyHb concentrations were calculated from the absorption coefficients of oxyHb and deoxyHb using the same law as that described in Sec. 2.4 with the assumption that background absorption is due to only 100% (by volume) water and that the refractive index of water is 1.3.

2.2 *Animal Study Protocol*

Eleven newborn piglets, less than 48 h old and weighing 1.9 to 2.4 kg, were each anesthetized with an intramuscular injection of sodium pentobarbital (2 mg/kg). The umbilical vein and artery of each piglet were cannulated. After cannulation, each piglet was paralyzed with pancronium bromide at an initial dose of 0.1 mg/kg followed by infusion at 0.1 $mg/kg\,h^{-1}$ and then anesthetized with fentanyl citrate at an initial dose of 10 μg/kg followed by infusion at 5 $\mu g/kg\,h^{-1}$. The animals were then intubated and mechanically ventilated with an infant ventilator. A 24-gauge cannula was inserted into the sagittal sinus through a burr hole in the anterior fontanel for venous blood sampling.

The umbilical artery was used for blood pressure monitoring and arterial blood sampling. Infusion of maintenance solution was continued at a rate of 4 $mL/kg\,h^{-1}$ via the umbilical vein. Respiration and acid-base balance were checked by arterial blood gas analysis at each step of FI_{O_2}. A negative base excess lower than 5.0 mmol/L, which was caused by hypoxia, was corrected as much as possible by sodium bicarbonate infusion to maintain *p*H between 7.3 and 7.5, thus minimizing the shift in the Hb dissociation curve. The hematocrit of arterial blood was in the normal range, and mean arterial pressure was maintained above 60 mm Hg except near zero FI_{O_2}. Arterial Hb oxygen saturation (SaO_2) and sagittal sinus venous Hb oxygen saturation (SvO_2) were measured using a blood co-oximeter (OSM-3, Radiometer, Copenhagen, Denmark). To obtain aerobic and anaerobic conditions, FI_{O_2} was changed by mixing pure nitrogen and oxygen gases with continuous monitoring by an oxygen electrode. We first set FI_{O_2} at 27% and then at 100% to obtain hyperaerobic conditions. Then, to obtain anaerobic conditions, FI_{O_2} was decreased in steps from 100 to 4%. The hair on the scalp of the parietal region was removed with an epilating agent. Two optical fibers were brought into contact with the skin on the head of each piglet. Throughout the experiment, rectal temperature was monitored and maintained between 38.0 and 39.0 °C using a heated-water mattress. At the end of the experiment, animals were sacrificed with intravenous pentobarbital (100 mg/kg). The protocols for animal care were in compliance with institutional guidelines.

2.3 *Near-IR TRS System and Analysis*

We used a portable three-wavelength TRS system (TRS-10, Hamamatsu Photonics K.K., Japan) and attached a probe to the head of each piglet with a light source fiber and light detector fiber separation of 30 mm. In the TRS system, a time-correlated single-photon-counting technique is used for detection. The system is controlled by a computer through a digital I/O interface consisting of a three-wavelength (761, 795, and 835 nm) picosecond light pulser (PLP) as the pulsed light source, a photon-counting head for single photon detec-

Table 1 Absorption coefficients for oxyHb, deoxyHb, water, and absorption of the piglet head with blood exchange transfusion by FC.

	oxyHb ($mM^{-1}\,cm^{-1}$)	deoxyHb ($mM^{-1}\,cm^{-1}$)	Water (cm^{-1})	Piglet Head with Blood Exchange Transfusion by FC (cm^{-1})
761 nm	1.418	3.841	0.0272	0.1190
795 nm	1.919	2.016	0.0214	0.1008
835 nm	2.487	1.798	0.0358	0.1260

tion, and signal-processing circuits for time-resolved measurement. The PLP emits NIR light with a pulse duration of about 100 ps and an average power of at least 150 μW at each wavelength at a repetition of 5 MHz, and the input light power to the subject was around 20 μW because of the loss in an incident optical system of the TRS system.

The light from the PLP is sent to a subject by a source fiber with a length of 3 m, and the photon reemitted from the subject is collected simultaneously by a detector fiber bundle with a length[29] of 3 m. The light source fiber was a graded index (GI) type single fiber (GC200/250L Fujikura, Japan) with a numerical aperture (NA) of 0.25 and a core diameter 200 μm, and the light detector fiber was a bundle fiber with a diameter of 3 mm and NA of 0.21. Finally, a set of histograms of the photon flight time, which is called a reemission profile, is recorded. One temporal reemission profile includes 1024 time channels spanning about 10 ns with a time step of about 10 ps. In this study, the emerging light was collected over a period of 3 s to exceed at least 1000 photon counts at the peak channel of the reemission profiles, and the procedure was repeated 30 times for each measurement.

The instrumental response was measured with the input fiber placed opposite the receiving fiber through a neutral density filter. The instrumental response of the TRS system was around 150 ps FWHM at each wavelength.

The mean optical path length was calculated from the difference between the center of gravity of the measured reemission profile and that of the instrumental response. It was assumed[30] that the value for the refractive index of brain tissue is 1.4.

The reemission profiles observed at each measurement point were fitted by the photon diffusion equation proposed by Patterson et al.[13] in order to calculate the values of absorption coefficient (μ_a) and reduced scattering coefficient (μ_s') of the head at wavelengths[18] of 761, 795, and 835 nm. In the fitting procedure, a nonlinear least-squares fitting method based on the Levenberg-Marquardt method was used. This is a method of iterative improvement. In each iterative calculation, the function from the photon diffusion equation in reflectance mode, which was convoluted with the instrumental response, was fitted to the observed reemission profile. The calculation regions were determined to include the observed profile data and the data of 600 channels were included into the fit.

2.4 *Estimation of Absolute Values of oxyHb and deoxyHb with Water-Only Background Absorption*

After determination of the values of μ_a at three wavelengths, the oxyHb and deoxyHb concentrations were calculated from the absorption coefficients of oxyHb and deoxyHb using the following equations with the assumption that background absorption is due only to 85% (by volume) water.[9,11]

$$\mu_{a\ 761\ \mathrm{nm}} = \varepsilon^{\mathrm{oxyHb}}_{761\ \mathrm{nm}}\,[\mathrm{oxyHb}] + \varepsilon^{\mathrm{deoxyHb}}_{761\ \mathrm{nm}}\,[\mathrm{deoxyHb}] + \varepsilon^{\mathrm{water}}_{761\ \mathrm{nm}}\,[\mathrm{water\ volume\ fraction}],$$

$$\mu_{a\ 795\ \mathrm{nm}} = \varepsilon^{\mathrm{oxyHb}}_{795\ \mathrm{nm}}\,[\mathrm{oxyHb}] + \varepsilon^{\mathrm{deoxyHb}}_{795\ \mathrm{nm}}\,[\mathrm{deoxyHb}] + \varepsilon^{\mathrm{water}}_{795\ \mathrm{nm}}\,[\mathrm{water\ volume\ fraction}],$$

$$\mu_{a\ 835\ \mathrm{nm}} = \varepsilon^{\mathrm{oxyHb}}_{835\ \mathrm{nm}}\,[\mathrm{oxyHb}] + \varepsilon^{\mathrm{deoxyHb}}_{835\ \mathrm{nm}}\,[\mathrm{deoxyHb}] + \varepsilon^{\mathrm{water}}_{835\ \mathrm{nm}}\,[\mathrm{water\ volume\ fraction}].$$

In these equations, $\varepsilon^{x}_{\lambda\ \mathrm{nm}}$ is the extinction coefficient at λ nm, and [oxyHb] and [deoxyHb] are the concentration.

First, the water absorption was subtracted from μ_a at each of the three wavelengths, and then the values of oxyHb and deoxyHb were estimated using the least-squares fitting method. The absorption coefficients for oxyHb, deoxyHb, and water shown in Table 1 were used.

The cerebral total hemoglobin (total Hb) concentration and cerebral Hb oxygen saturation (SO_2) were calculated as follows:

$$[\mathrm{total\ Hb}] = [\mathrm{oxyHb}] + [\mathrm{deoxyHb}],$$

$$SO_2\ (\%) = [\mathrm{oxyHb}]/([\mathrm{oxyHb}] + [\mathrm{deoxyHb}]) \times 100,$$

where the square brackets indicate concentration.

2.5 *Estimation of Absolute Values of oxyHb and deoxyHb with Absorption of the Piglet Head with Blood Exchange Transfusion by FC*

For measurement of background absorption of the head without Hb, we used a piglet for blood exchange transfusion by FC. First, partial blood exchange was done by saline and then blood was replaced with perfluorotributylamine emulsion (FC43 Emulsion, Green Cross Corp., Japan) as an oxygen carrier. We used 500 mL of FC and the hematocrit was lowered to 0.5%. After replacing the blood with FC, oxygenated head TRS measurements were done while the piglet breathed 100% O_2. The EEG showed normal activity during the period of ventilation with 100% O_2. We used the μ_a of piglet head with blood exchange transfusion by FC at three wavelengths as the background absorption value. The values at 761, 795, and 835 nm were estimated to be 0.1190, 0.1008, and 0.1260,

respectively (Table 1). The following equations were used for estimation of oxyHb and deoxyHb concentrations:

$$\mu_{a\ 761\ \mathrm{nm}} = \varepsilon^{\mathrm{oxyHb}}_{761\ \mathrm{nm}}\ [\mathrm{oxyHb}] + \varepsilon^{\mathrm{deoxyHb}}_{761\ \mathrm{nm}}\ [\mathrm{deoxyHb}] + \mu_{a\ 761\ \mathrm{nm}}^{\mathrm{background}},$$

$$\mu_{a\ 795\ \mathrm{nm}} = \varepsilon^{\mathrm{oxyHb}}_{795\ \mathrm{nm}}\ [\mathrm{oxyHb}] + \varepsilon^{\mathrm{deoxyHb}}_{795\ \mathrm{nm}}\ [\mathrm{deoxyHb}] + \mu_{a\ 795\ \mathrm{nm}}^{\mathrm{background}},$$

$$\mu_{a\ 835\ \mathrm{nm}} = \varepsilon^{\mathrm{oxyHb}}_{835\ \mathrm{nm}}\ [\mathrm{oxyHb}] + \varepsilon^{\mathrm{deoxyHb}}_{835\ \mathrm{nm}}\ [\mathrm{deoxyHb}] + \mu_{a\ 835\ \mathrm{nm}}^{\mathrm{background}}.$$

In these equations, $\mu_{a\ \lambda\ \mathrm{nm}}^{\mathrm{background}}$ is the background absorption derived from the piglet head with blood exchange transfusion by FC. First, the absorption of the head with blood exchange transfusion by FC (abs of the head with BET by FC) was subtracted from μ_a at each of the three wavelengths, and then the values of oxyHb and deoxyHb were estimated using the least-squares fitting method.

2.6 *Statistical Analysis*

A Statview J 4.5 package for the Macintosh computer was used for statistical analysis. Values obtained at different levels of FI_{O_2} were compared from values at FI_{O_2} of 21% by Wilcoxon's signed-rank test. The level of statistical significance was set at a probability of $p<0.05$ for all tests. Results at FI_{O_2} levels in the range 10 to 100% were obtained from measurements in 11 piglets, results at FI_{O_2} of 8 and 6% were obtained from 10 piglets and results at FI_{O_2} of 4% were obtained from 8 piglets. Values are expressed as means ± standard deviation (SD).

3 Results

3.1 *In Vitro Experiment Results*

Figure 1(a) shows the relationship between the actual blood volume and total Hb concentration of the model as measured by TRS. The relationship between the actual blood volume (X) and Hb concentration measured by TRS (Y) was $Y=0.843X+2.21$ ($r=0.998$, $P<0.001$). We can see that the relationship between these two parameters is linear over the experimental range of Hb concentrations. Figure 1(b) shows the relationship between the values of Hb oxygen saturation in the 80-μM Hb suspension measured by a conventional gas analyzer or TRS. The relationship between the values of Hb oxygen saturation measured by a conventional gas analyzer (X) and TRS (Y) was $Y=0.960X+0.889$ ($r=0.991$, $P<0.001$). Linear regression analysis demonstrated that a significant correlation existed between the respective values determined by the two methods. These results indicated that our TRS method enables accurate and noninvasive measurement of Hb content and oxygen saturation in a highly scattered medium such as the piglet brain.

3.2 *Values of μ_s' and μ_a*

In Fig. 2, the values of μ_s' measured concurrently at corresponding FI_{O_2} levels are plotted against FI_{O_2}. At FI_{O_2} of 21%, the values of μ_s' of the newborn piglet brain at 761, 795, and 835 nm were estimated to be 8.70±1.23, 8.33±0.91, and 8.24 ±1.11/cm, respectively. There were no significant differences between the values of μ_s' for each FI_{O_2} level in the range of 4 to 100% at all three wavelengths.

In Fig. 3, the values of μ_a' measured concurrently at corresponding FI_{O_2} levels are plotted against FI_{O_2}. The values of μ_a at 761 and 795 nm at FI_{O_2} levels below 15% were higher than the values at FI_{O_2} of 21% at each wavelength. When FI_{O_2} was decreased from 21 to 15%, the values of μ_a at 761 and 795 nm increased from 0.227±0.021 to 0.259±0.024/cm and from 0.189±0.016 to 0.203±0.013/cm, respectively. The values of μ_a at 835 nm at FI_{O_2} levels below 10% were higher than those at an FI_{O_2} level of 21%. When FI_{O_2} was decreased from 21 to 10%, the value of μ_a at 835 nm increased from 0.223±0.020 to 0.251±0.025/cm.

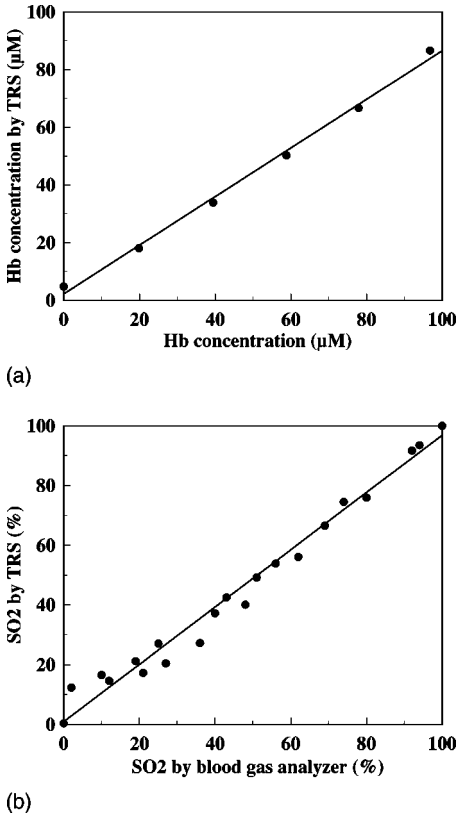

Fig. 1 (a) Relationship between actual blood volume and total Hb concentration of the model as measured by TRS. The relationship between actual blood volume (X) and Hb concentration measured by TRS (Y) was $Y=0.843X+2.21$ ($r=0.998$, $P<0.001$). (b) Relationship between values of Hb oxygen saturation in the 80-μM Hb suspension measured by a conventional gas analyzer and by TRS. The relationship between values of Hb oxygen saturation measured by a conventional gas analyzer (X) and by TRS (Y) was $Y=0.960X+0.889$ ($r=0.991$, $P<0.001$).

3.3 *Concentration of oxyHb and deoxyHb with Water-Only Background Absorption*

As shown in Fig. 4(a), the relationship between oxyHb and deoxyHb changed reciprocally in a mirror-image manner

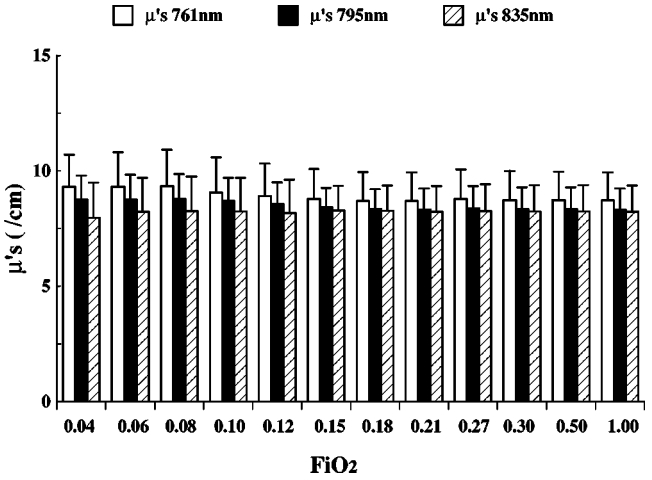

Fig. 2 Values of μ_s' at 761, 795, and 835 nm, which were measured concurrently at corresponding FI_{O_2} levels, are presented as a function of FI_{O_2}. The error bars show 1 SD of the mean. At FI_{O_2} of 21%, values of μ_s' in the newborn piglet head at 761, 795, and 835 nm were estimated to be 8.70±1.23 (mean±SD), 8.33±0.91, and 8.24±1.11/cm, respectively.

when FI_{O_2} was changed. Total Hb showed an increase of 31.3% when FI_{O_2} was decreased from 21 to 6%, indicating that cerebral blood volume increased during hypoxia. The values of oxyHb, deoxyHb, and total Hb at FI_{O_2} of 21% were 53.5±8.1, 33.4±5.8, and 86.9±8.1 μM, respectively.

In Fig. 5(a), levels of SO_2, SaO_2, and SvO_2, which were measured concurrently at corresponding FI_{O_2} levels, are plotted against FI_{O_2}. At FI_{O_2} of 21%, the mean SO_2 of newborn piglets was calculated to be 61.5±6.3%. The values of SaO_2 and SvO_2 were simultaneously determined to be 92.1±3.76

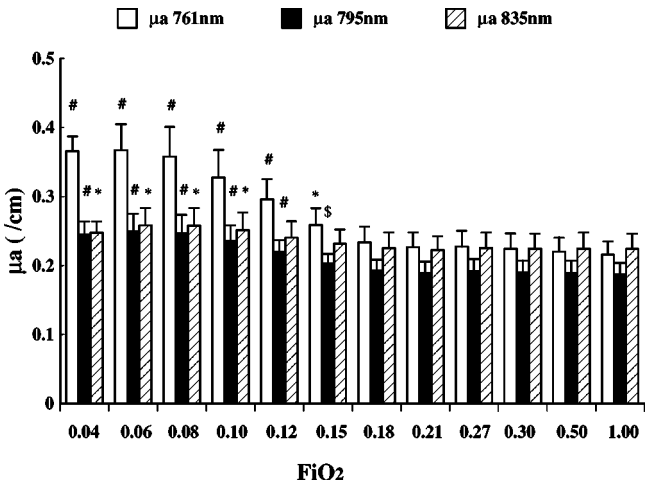

Fig. 3 Values of μ_a at 761, 795, and 835 nm, which were measured concurrently at corresponding FI_{O_2} levels, are presented as a function of FI_{O_2}. The error bars show 1 SD of the mean. At FI_{O_2} of 21%, values of μ_a in the newborn piglet head at 761, 795, and 835 nm were estimated to be 0.227±0.021 (mean±SD), 0.189±0.016, and 0.223 ±0.020/cm, respectively. Here, #, $P<0.001$; *, $P<0.01$; and \$, $P<0.05$, indicate significant differences from values at FI_{O_2} of 21% using Wilcoxon's signed-rank test.

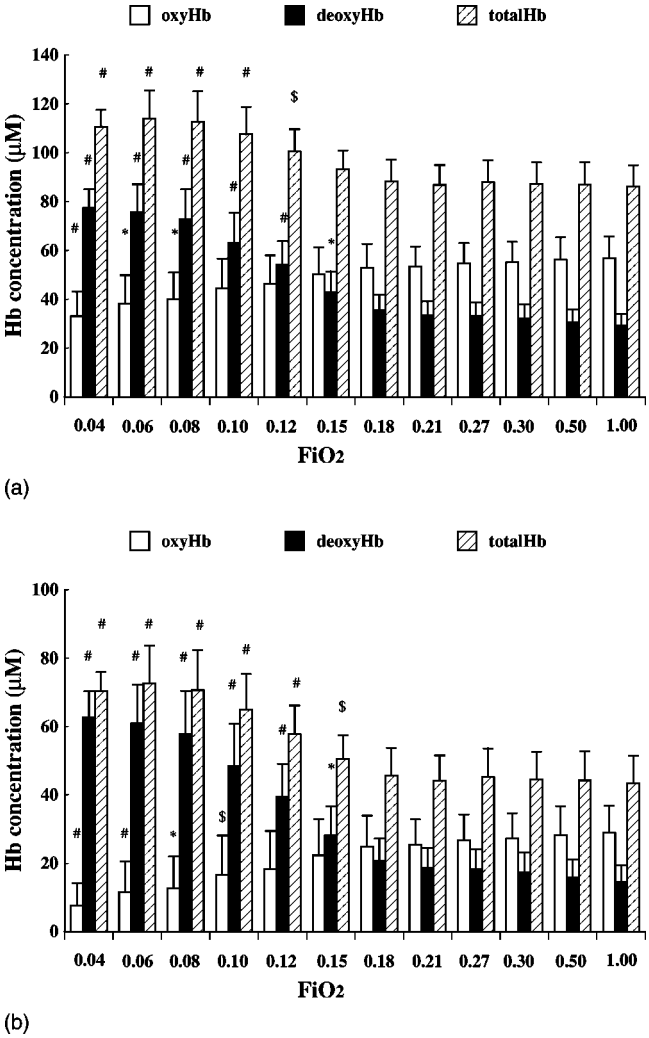

Fig. 4 Concentrations of oxyHb, deoxyHb, and total Hb, which were measured concurrently at corresponding FI_{O_2} levels, are presented as a function of FI_{O_2}. The error bars show 1 SD of the mean. (a) Using the water-only background absorption, at FI_{O_2} of 21%, oxyHb, deoxyHb, and total Hb concentrations in the newborn piglet head were estimated to be 53.5±8.1 (mean±SD), 33.4±5.8, and 86.9±8.1 μM, respectively. (b) Using absorption of the piglet head with blood exchange transfusion by FC, at FI_{O_2} of 21%, oxyHb, deoxyHb, and total Hb concentrations in the newborn piglet head were estimated to be 25.5±7.3, 18.6±5.8, and 44.1±7.4 μM, respectively. Here, #, $P<0.001$; *, $P<0.01$; and \$, $P<0.05$, indicate significant differences from values at FI_{O_2} of 21% using Wilcoxon's signed-rank test.

and 40.1±6.4%, respectively. The contributions of SaO_2 and SvO_2 to SO_2 were 41.1 and 58.9%, respectively. However, values of SO_2 at FI_{O_2} in the range of 10 to 4% were higher than those of SaO_2.

The SaO_2 values also showed a positive linear relationship with SO_2 [Fig. 6(a)]. The relationship between SaO_2 and SO_2 was $SO_2 = 37.9 \times 10^{-2} \times SaO_2 + 27.5$ ($r = 0.862$, $P < 0.001$). From this regression equation, the values of SaO_2 and SO_2 were estimated to be 44.3% when SO_2 was larger than SaO_2 during a hypoxic condition.

As shown in Fig. 7(a), there was a positive linear relationship between SvO_2 and SO_2. The relationship between SvO_2

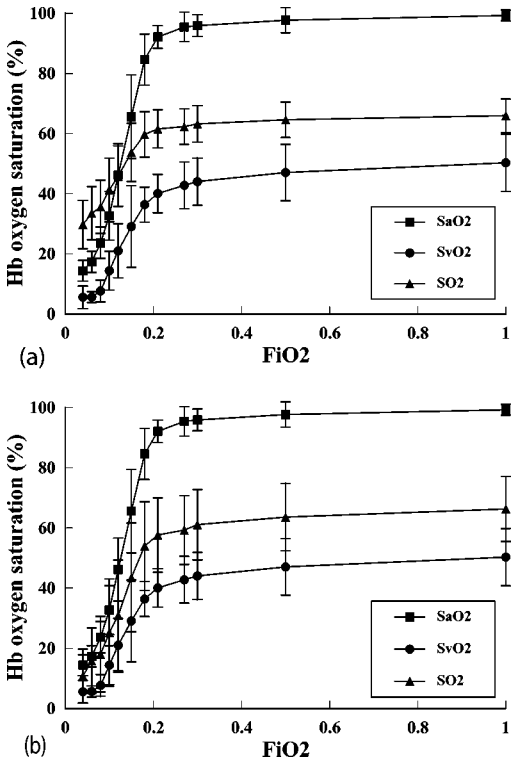

Fig. 5 Comparison of changes in SO_2 in the brain, SaO_2 in the artery, and SvO_2 in the internal jugular vein during loading with stepwise decrease in FI_{O_2} using (a) water-only background absorption and (b) absorption of the piglet head with blood exchange transfusion by FC.

and SO_2 was $SO_2 = 69.3 \times 10^{-2} \times SvO_2 + 31.8$ ($r = 0.841$, $P < 0.001$).

3.4 *Concentration of oxyHb and deoxyHb with Absorption of the Piglet Head with Blood Exchange Transfusion by Fluorocarbon*

As shown in Fig. 4(b), the relationship between oxyHb and deoxyHb changed reciprocally in a mirror-image manner when FI_{O_2} was changed. The values of oxyHb, deoxyHb, and total Hb at FI_{O_2} of 21% were 25.5±7.3, 18.6±5.8, and 44.1 ±7.4 μM, respectively. The values of oxyHb, deoxyHb, and total Hb are significantly lower at each FI_{O_2} level than those in the case of water-only background absorption.

In Fig. 5(b), levels of SO_2, SaO_2, and SvO_2, which were measured concurrently at corresponding FI_{O_2} levels, are plotted against FI_{O_2}. At FI_{O_2} of 21%, the mean SO_2 of newborn piglets was calculated to be 57.6±12.3%. The contributions of SaO_2 and SvO_2 to SO_2 were 33.7 and 66.3%, respectively. SO_2 values were between those of SaO_2 and SvO_2 at all levels of FI_{O_2}. SO_2 values are not significantly different from SO_2 values using the water-only background at FI_{O_2} in the range of 15 to 100%, but the values are lower than the values using the water-only background at FI_{O_2} in the range of 4 to 12%.

The SaO_2 values also showed a positive linear relationship with SO_2 [Fig. 6(b)]. The relationship between SaO_2 and SO_2 was $SO_2 = 59.0 \times 10^{-2} \times SaO_2 + 4.9$ ($r = 0.843$, $P < 0.001$).

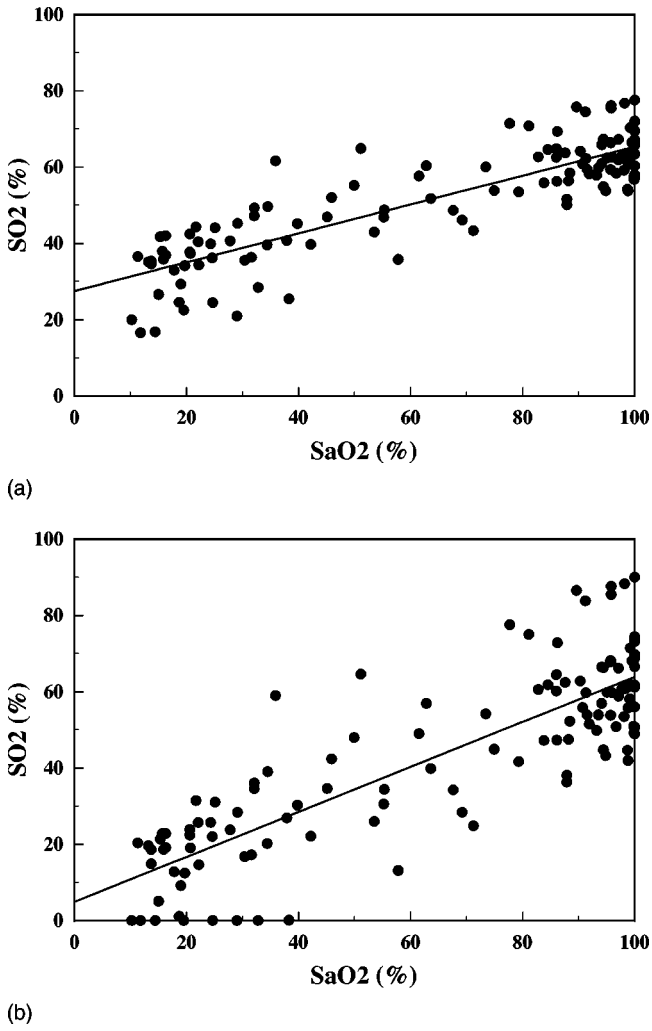

Fig. 6 Relationships between SO_2 and SaO_2 at various oxygenation levels: (a) using the water-only background absorption, the relationship between SO_2 and SaO_2 was $SO_2 = 37.9 \times 10^{-2} \times SaO_2 + 27.5$ ($r = 0.862$, $P < 0.001$), and (b) using absorption of the piglet head with blood exchange transfusion by FC, the relationship between SaO_2 and SO_2 was $SO_2 = 59.0 \times 10^{-2} \times SaO_2 + 4.9$ ($r = 0.843$, $P < 0.001$).

As shown in Fig. 7(b), there was a positive linear relationship between SvO_2 and SO_2. The relationship between SvO_2 and SO_2 was $SO_2 = 108.6 \times 10^{-2} \times SvO_2 + 11.5$ ($r = 0.829$, $P < 0.001$).

4 Discussion

Cerebral Hb content and Hb oxygen saturation in infants have already been estimated using NIRS in several studies. However, the values estimated in those studies cannot be compared easily because the same phantom models, animal models, and experimental protocols were not used in those studies. Although the ultimate purpose of this study was to estimate SO_2 and Hb content in infants, cerebral Hb content and SO_2 have already been estimated by NIRS in previous studies using an experimental animal model, i.e., the newborn piglet, which approximates infants. The NIRS used in those studies can be divided into three categories: (1) FSS (Refs. 11 and 12), (2) PMS (Refs. 20, 22, 23, 25, and 31), and (3) TRS (Ref. 17).

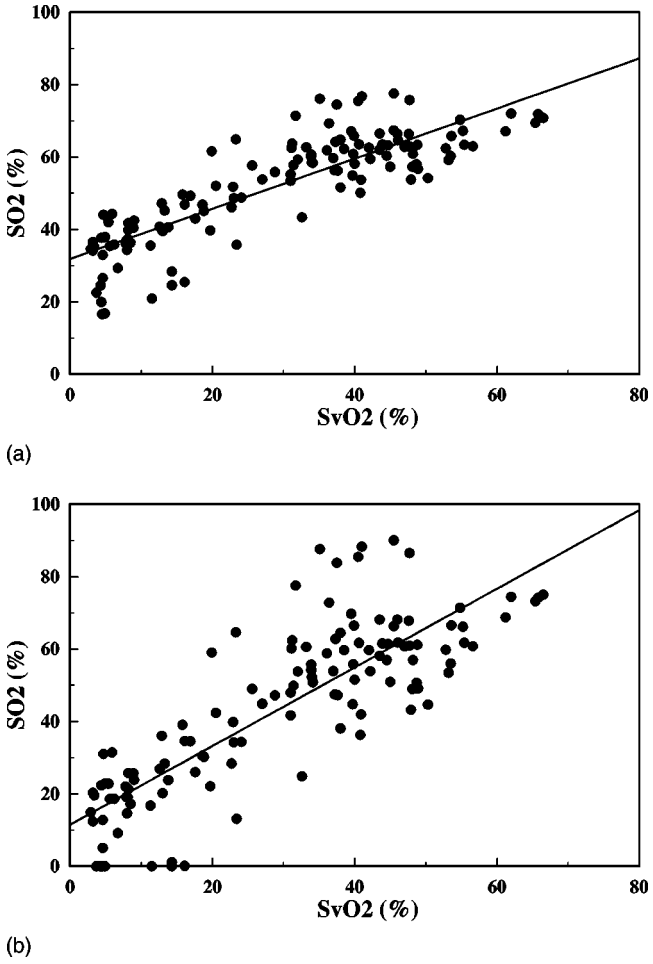

Fig. 7 Relationships between SO_2 and SvO_2 at various oxygenation levels: (a) using the water-only background absorption, the relationship between SO_2 and SvO_2 was $SO_2 = 69.3 \times 10^{-2} \times SvO_2 + 31.8$ ($r = 0.841, P < 0.001$), and (b) using absorption of the piglet head with blood exchange transfusion by FC, the relationship between SvO_2 and SO_2 was $SO_2 = 108.6 \times 10^{-2} \times SvO_2 + 11.5$ ($r = 0.829, P < 0.001$).

Therefore, we used newborn piglets with hypoxia for our study to investigate the validity of NIR TRS. This model is easy to reproduce and is useful for comparison with results obtained by using other methods.

In the *in vitro* study, the use of intralipids and blood phantom showed that qualitative measurements of Hb concentrations and of oxygen saturation could be made under the same conditions as those in an *in vivo* study. The Hb concentration used was approximately the same as the Hb molar concentration in the human brain. Even if the dispersion of light is the same as that for a human brain, quantitative analysis of Hb concentration and oxygenation is considered possible. In practice, however, there is a substantial difference between this model and noninvasive measurement of head structure: the head has a multiplex structure, and blood vessels have an inhomogenous structure.

The application of an analytical solution of the diffusion equation assumes a homogeneous medium, but the piglet head consists of multilayers including the scalp, skull, cerebrospinal fluid (CSF) layer, gray matter, and white matter. The optical fibers were attached to the skin. Therefore, the obtained optical properties are not those of only the brain but the average of those of the multiple layers.

Kienle et al.[32,33] investigated analytical solutions to the two-layered optical phantom model using the PMS method. They demonstrated that a superficial layer of 4 mm in thickness (or less) will have only a small influence on the accuracy of the measured optical properties of an underlying thick layer. In the piglets used in our study, the thickness of the scalp and skull layer measured postmortem were about 1.5 and 1.5 mm, respectively, similar to values obtained in an earlier study.[24,25] Huber et al.[24] and Fantini et al.[25] concluded that in the presence of a relatively thin ($\leqslant$4 mm) scalp/skull layer (as in the case of the neonatal piglet), those absolute values of Hb concentration and oxygen saturation should be actually representative of the brain. In contrast, the significantly thicker tissue inhomogeneities found in the adult human head have an effect on the absolute optical measurements.

Furthermore, with regard to the effect of the CSF layer on photon migration, Fukui et al.[34] estimated light properties from results of Monte Carlo simulation using the neonatal head model. In their model, the thicknesses of the scalp, skull, and CSF layer were about 2, 2, and 1 mm, respectively, almost the same as the values in our piglet model. A photon that has penetrated into the white matter can be identified by a detector 10 mm from the source. The partial DPF for the white matter proportionally increased with the increase in source-detector spacing, whereas that for the gray matter was almost constant at source-detector spacing greater than 30 mm. At source-detector spacing of 30 mm, the DPF was almost 4.3 and the values of partial DPF of gray matter and white matter were 1.3 and 0.7, respectively. Fukui et al.[34] reported that the intensity sensitive region in the neonatal brain is confined to the gray matter, but the spatial sensitivity profile penetrates into the deeper region of the white matter. Therefore, our TRS measurements of the piglet head enable estimation of Hb of the brain, which is a multilayer structure, and the contribution of the brain to the measurement signal is estimated to be approximately 50%. If the contributions of the scalp, skull, and CSF layers of the measurement signal are assumed to be 10, 20, and 20%, respectively,[35] and μ_a values of the scalp, skull, and CSF at 795 nm are assumed to be 0.18, 0.16, and 0.04/cm, respectively,[34] the μ_a of the brain is estimated to be 0.24/cm. This value is lower than that of the human neonatal brain gray or white matter.[32]

There were no significant differences between the values of μ_s' at each wavelength for FI_{O_2} levels in the range of 4 to 100%. These results are similar to those obtained in a study by Zhang et al.,[36] showing that scattering changes detected by a frequency-domain oximeter were associated only with asphyxia and death. Yamashita et al.[37] reported the results of a preliminary study on light scattering in the piglet brain by using TRS. Their results showed that the values of μ_s' in piglet brains were around 1.3 mm^{-1} in a state of normoxia and that the value of μ_s' showed a notable decrease after death. Tissue edema and structural changes occur during severe hypoxia, particularly at and after death, and values of μ_s' are thought to change only during structural changes in tissue due to cerebral energy failure. Therefore, there were no sig-

Table 2 Values of cerebral Hb oxygen saturation (SO_2) and Hb concentration (total Hb) in the piglet head in a state of normoxia measured by using near-infrared spectroscopy.

Methods	Number of Subjects	Age	SO_2 (%)	Total Hb (μM)	References
FSS	7	less than 24 h	65.4±3.5	37.5±9.1	Springett et al.[11]
FSS	5	5 to 6 weeks	48.4±3.2		Sakamoto et al.[10]
FSS	8	less than 24 h	63±4		Kusaka et al.[12]
PMS	60	5 to 10 days	68±5		Kurth et al.[23]
PMS	12	1 to 2 days	84		Du et al.[22]
PMS	4		58.5±2	63±14	Hueber et al.[24]
PMS	3	11±1 days	60	42	Fantini et al.[25]
TRS	6	2 to 5 days		138±31	Kurth and Uher[16]
TRS	1	2 weeks	65	110	Yamashita et al.[17]
TRS	11	less than 48 h	57.6±12.3	44.1±7.4	Ijichi et al. (this paper)

FSS, full spectral spectroscopy; PMS, phase-modulated spectroscopy; TRS, time-resolved spectroscopy.

nificant differences between the values of μ_s' during hypoxia in this study.

The values μ_a at 761 and 795 nm at FI_{O_2} levels below 15% were significantly higher than those at FI_{O_2} of 21% at each wavelength because deoxyHb increased during hypoxia. The values of μ_a at 835 nm at FI_{O_2} levels below 10% were higher than those at an FI_{O_2} of 21%. This is because of an increase in both oxyHb and deoxyHb absorption, indicating an increase in cerebral blood volume during hypoxia.

In this paper, at levels of FI_{O_2} in the range of 10 to 4%, the values of SO_2 using a water-only background were higher than those of SaO_2 [Fig. 4(a)]. These results are thought to be mainly due to the effect of background absorption in tissue.[24] In the brain, Hb, water, and cytochrome *c* oxidase are known chromophores in the NIR region,[38] but the concentrations vary between individuals and the *in vivo* absorption spectra of cytochromes are difficult to measure precisely. It is also likely that there are other important chromophores, such as fats, that make a significant contribution to non-Hb absorption. Indeed, Hueber et al.[24] reported that using the frequency-domain multidistance method in the piglet head, SO_2 is greater than SaO_2 under the condition of extreme hypoxia with the assumption of a water-only background. They estimated the background tissue absorption with the assumption that SO_2 is equivalent to a mixture of 50% SaO_2 and 50% SvO_2 during normoxia and mild hypoxia to improve the estimation of brain Hb.

In this paper, we estimated the background absorption from the piglet head with blood exchange transfusion by FC. Using this absorption, the Hb values were lower than those using a water-only background, especially at a low level of FI_{O_2}. The SO_2 values obtained using abs of the head with BET by FC were between the values of SaO_2 and SvO_2. These values were more accepted from a physiological point of view.

The mean SO_2 in 11 newborn piglets at FI_{O_2} of 21% was calculated to be 58% using FC blood exchanged piglet head absorption. The values of SaO_2 and SvO_2 were simultaneously determined to be 92 and 40%, respectively. The contributions from arterial blood and venous blood were estimated to be 34 and 66%, respectively. The ratio of the contribution of arterial blood to that of venous blood is almost the same as the ratios reported by Brun et al.[39] and Kusaka et al.[12] Thus, the validity of measurement *in vivo* can be verified, even in an inhomogenous piglet head. Table 2 shows some values of cerebral Hb content and SO_2 in newborn piglets measured by using NIRS. Previously reported values of[10,11,17,22–25] SO_2 in newborn piglets range from 48 to 84%, a range similar to our results.

In conclusion, the results of this study demonstrated that our NIR TRS method can be used to monitor cerebral Hb oxygen saturation and Hb content in a piglet model, especially using abs of the head with BET by FC. However, more studies are required for estimation of true background absorption and for developing and validating the instrument for clinical use.

Acknowledgments

We thank Mr. M. Oda, Mr. Y. Yamashita, and Hamamatsu Photonics, K.K., for their technical support in this study. This study was supported by grants-in-aid for scientific research (C), Nos. 13671140, 14571051, and 15591159, and encouragement of young scientists, Nos. 13770619 and 14770571, from the Ministry of Education, Culture, Sports, Science and Technology of Japan.

References

1. J. E. Brazy, D. W. Lewis, M. H. Mitnick, and F. F. Jobsis, ''Noninvasive monitoring of cerebral oxygenation in preterm infants: preliminary observations,'' *Pediatrics* **75**, 217–225 (1985).
2. J. S. Wyatt, M. Cope, D. T. Delpy, S. Wray, and E. O. R. Reynolds, ''Quantification of cerebral oxygenation and haemodynamics in sick newborn infants by near infrared spectrophotometry,'' *Lancet* **ii**, 1063–1066 (1986).
3. A. D. Edwards, J. S. Wyatt, C. Richardson, D. T. Delpy, M. Cope, and E. O. R. Reynolds, ''Cotside measurement of cerebral blood flow in ill newborn infants by near infrared spectroscopy,'' *Lancet* **ii**, 770–771 (1988).
4. K. D. Liem, J. C. Hopman, B. Oeseburg, A. F. de Haan, C. Festen, and L. A. Kollee, ''Cerebral oxygenation and hemodynamics during

induction of extracorporeal membrane oxygenation as investigated by near infrared spectrophotometry,'' *Pediatrics* **95**, 555–561 (1995).
5. O. Pryds, G. Greisen, L. L. Skov, and B. F. Hansen, ''Carbon dioxide-related changes in cerebral blood volume and cerebral blood flow in mechanically ventilated preterm neonates: comparison of near infrared spectrophotometry and ^{133}Xenon clearance,'' *Pediatr. Res.* **27**, 445–449 (1990).
6. F. van Bel, C. A. Dorrepaal, M. J. Benders, P. E. Zeeuwe, M. van der Bor, and H. M. Berger, ''Changes in cerebral hemodynamics and oxygenation in the first 24 hours after birth asphyxia,'' *Pediatrics* **92**, 365–372 (1993).
7. C. W. Yoxall, A. M. Weindling, N. H. Dawani, and I. Peart, ''Measurement of cerebral venous oxyhemoglobin saturation in children by near-infrared spectroscopy and partial jugular venous occlusion,'' *Pediatr. Res.* **38**, 319–323 (1995).
8. S. Nioka, B. Chance, D. S. Smith, A. Mayevsky, M. P. Reilly, C. Alter, and T. Asakura, ''Cerebral energy metabolism and oxygen state during hypoxia in neonate and adult dogs,'' *Pediatr. Res.* **28**, 54–62 (1990).
9. C. E. Cooper, C. E. Elwell, J. H. Meek, S. J. Matcher, J. S. Wyatt, M. Cope, and D. T. Delpy, ''The noninvasive measurement of absolute cerebral deoxyhemoglobin concentration and mean optical path length in the neonatal brain by second derivative near infrared spectroscopy,'' *Pediatr. Res.* **39**, 32–38 (1996).
10. T. Sakamoto, R. A. Jonas, U. A. Stock, S. Hatsuoka, M. Cope, R. Springett, and G. Nollert, ''Utility and limitations of near-infrared spectroscopy during cardiopulmonary bypass in a piglet model,'' *Pediatr. Res.* **49**, 770–776 (2001).
11. R. Springett, J. Newman, M. Cope, and D. T. Delpy, ''Oxygen dependency and precision of cytochrome oxidase signal from full spectral NIRS of the piglet brain,'' *Am. J. Physiol. Heart Circ. Physiol.* **279**, 2202–2209 (2000).
12. T. Kusaka, K. Isobe, K. Nagano, K. Okubo, S. Yasuda, M. Kondo, S. Itoh, K. Hirao, and S. Onishi, ''Quantification of cerebral oxygenation by full-spectrum near-infrared spectroscopy using a two-point method,'' *Comp. Biochem. Physiol. A* **132**, 121–132 (2002).
13. M. S. Patterson, B. Chance, and B. Wilson, ''Time resolved reflectance and transmittance for the non-invasive measurement of optical properties,'' *Appl. Opt.* **289**, 2331–2336 (1989).
14. E. M. Sevick, B. Chance, J. Leigh, S. Nioka, and M. Maris, ''Quantitation of time- and frequency-resolved optical spectra for the determination of tissue oxygenation,'' *Anal. Biochem.* **195**, 330–351 (1991).
15. B. Chance, J. S. Leigh, H. Miyake, D. S. Smith, S. Nioka, R. Greenfeld, M. Finander, K. Kaufmann, W. Levy, M. Young, P. Cohen, H. Yoshioka, and R. Boretsky, ''Comparison of time-resolved and -unresolved measurements of deoxyhemoglobin in brain,'' *Proc. Natl. Acad. Sci. U.S.A.* **85**, 4971–4975 (1988).
16. C. D. Kurth and B. Uher, ''Cerebral hemoglobin and optical pathlength influence near-infrared spectroscopy measurement of cerebral oxygen saturation,'' *Anesth. Analg. (Baltimore)* **84**, 1297–1305 (1997).
17. Y. Yamashita, M. Oda, E. Ohmae, and M. Tamura, ''Continuous measurement of oxy- and deoxyhemoglobin of piglet brain by time-resolved spectroscopy,'' in *OSA TOPS*, Vol. 22, *Biomedical Optical Spectroscopy and Diagnostics/Therapeutic Laser Applications*, pp. 205, 207, Optical Society of America, Washington, DC (1998).
18. M. Oda, Y. Yamashita, T. Nakano, A. Suzuki, K. Shimizu, I. Hirno, F. Shimomura, E. Ohmae, T. Suzuki, and T. Tsuchiya, ''Nearinfrared time-resolved spectroscopy system for tissue oxygenation monitor,'' *Proc. SPIE* **3597**, 611–617 (1999).
19. E. Gratton, S. Fantini, M. Franceschini, and J. B. Fishkin, ''Near infrared optical spectroscopy of tissue using an LED frequency domain spectrometer,'' in *Advances in Optical Imaging and Photon Migration, Technical Digest*, pp. 212–215, Optical Society of America, Washington, DC (1994).
20. H. Y. Ma, Q. Xu, J. R. Ballesteros, V. Ntziachristos, Q. Zhang, and B. Chance, ''Quantitative study of hypoxia stress in piglet brain by IQ phase modulation oximetry,'' *Proc. SPIE* **3597**, 642–649 (1999).
21. M. A. Franceschini, D. A. Boas, A. Zourabian, S. G. Diamond, S. Nadgir, D. W. Lin, J. B. Moore, and S. Fantini, ''Near-infrared spiroximetry: noninvasive measurements of venous saturation in piglets and human subjects,'' *J. Appl. Physiol.* **92**, 372–384 (2002).
22. C. Du, C. Andersen, and B. Chance, ''Quantitative detection of hemoglobin saturation on piglet brain by near-infrared frequency-domain spectroscopy,'' *Proc. SPIE* **3194**, 55–62 (1998).
23. C. D. Kurth, W. J. Levy, and J. McCann, ''Near-infrared spectroscopy cerebral oxygen saturation thresholds for hypoxia-ischemia in piglets,'' *J. Cereb. Blood Flow Metab.* **22**, 335–341 (2002).
24. D. M. Hueber, M. A. Franceschini, H. Y. Ma, Q. Zhang, J. R. Ballesteros, S. Fantini, D. Wallace, V. Ntziachristos, and B. Chance, ''Non-invasive and quantitative near-infrared haemoglobin spectrometry in the piglet brain during hypoxic stress, using a frequency-domain multidistance instrument,'' *Phys. Med. Biol.* **46**, 41–62 (2001).
25. S. Fantini, D. Hueber, M. A. Franceschini, E. Gratton, W. Rosenfeld, P. G. Stubblefield, D. Maulik, and M. R. Stankovic, ''Non-invasive optical monitoring of the newborn piglet brain using continuous-wave and frequency-domain spectroscopy,'' *Phys. Med. Biol.* **44**, 1543–1563 (1999).
26. S. Suzuki, S. Takasaki, T. Ozaki, and Y. Kobayashi, ''A tissue oxygenation monitor using NIR spatially resolved spectroscopy,'' *Proc. SPIE* **3597**, 582–592 (1999).
27. T. Kusaka, Y. Hisamatsu, K. Kawada, K. Okubo, H. Okada, M. Namba, T. Imai, K. Isobe, and S. Itoh, ''Measurement of cerebral optical pathlength as a function of oxygenation using near-infrared time-resolved spectroscopy in a piglet model of hypoxia,'' *Opt. Rev.* **10**, 466–469 (2003).
28. S. Ijichi, T. Kusaka, K. Okubo, K. Kawada, T. Imai, K. Isobe, and S. Itoh, ''Quantitative time-resolved near-infrared spectroscopy measurement of muscle oxygenation for arterial thrombosis in infant'' [abstract], *J. Perinat. Med.* **31**, 258 (2003).
29. A. Liebert, H. Wabnitz, D. Grosenick, and R. Macdonald, ''Fiber dispersion in time domain measurements compromising the accuracy of determination of optical properties of strongly scattering media,'' *J. Biomed. Opt.* **8**, 512–516 (2003).
30. P. F. Bolin, L. E. Preuss, R. C. Taylor, and R. J. Ference, ''Refractive index of some mammalian tissues using a fiber optic cladding method,'' *Appl. Opt.* **28**, 2297–2303 (1989).
31. M. R. Stankovic, D. Maulik, W. Rosenfels, P. G. Stubblefield, A. D. Kofinas, S. Drexler, R. Nair, M. A. Franceschini, D. Hueber, E. Gratton, and S. Fantini, ''Real-time optical imaging of experimental brain ischemia and hemorrhage in neonatal piglets,'' *J. Perinat. Med.* **27**, 279–286 (1999).
32. A. Kienle, T. Glanzmann, G. Wagnieres, and H. van der Bergh, ''Investigation of two-layered turbid media with time-resolved reflectance,'' *Appl. Opt.* **37**, 6852–6862 (1998).
33. A. Kienle, M. S. Patterson, N. Dognitz, R. Bays, G. Wagnieres, and H. van der Bergh, ''Noninvasive determination of the optical properties of two-layered turbid media,'' *Appl. Opt.* **37**, 779–791 (1998).
34. Y. Fukui, Y. Ajichi, and E. Okada, ''Monte Carlo prediction of near-infrared light propagation in realistic adult and neonatal head models,'' *Appl. Opt.* **42**, 2881–2887 (2003).
35. E. Okada and D. T. Delpy, ''The effect of overlying tissue on nir light in neonatal brain,'' in *OSA TOPS, Advances in Optical Imaging and Photon Migration*, R. R. Alfano and G. J. Fujimoto, Eds., Vol. 2, pp. 387–390, Optical Society of America, Washington, DC (1996).
36. G. Zhang, A. Katz, R. R. Alfano, A. D. Kofinas, D. A. Kofinas, P. G. Stubblefield, W. Rosenfeld, D. Beyer, D. Maulik, and M. R. Stankovic, ''Brain perfusion monitoring with frequency-domain and continuous-wave near-infrared spectroscopy: a cross-correlation study in newborn piglets,'' *Phys. Med. Biol.* **45**, 3143–3158 (2000).
37. Y. Yamashita, M. Oda, H. Naruse, and M. Tamura, ''In vivo measurement of reduced scattering and absorption coefficients of living tissue using time-resolved spectroscopy,'' in *OSA TOPS, Advances in Optical Imaging and Photon Migration*, R. R. Alfano and G. J. Fujimoto, Eds., Vol. 2, pp. 387–390, Optical Society of America, Washington, DC (1996).
38. S. J. Matcher, C. E. Elwell, C. E. Cooper, M. Cope, and D. T. Delpy, ''Performance comparison of several published tissue near-infrared spectroscopy algorithms,'' *Anal. Biochem.* **227**, 54–68 (1995).
39. N. C. Brun, A. Moen, K. Borch, O. D. Saugstad, and G. Greisen, ''Near infrared monitoring of cerebral tissue oxygen saturation and blood volume in newborn piglets,'' *Am. J. Physiol.* **273**, 682–686 (1997).